Thermal transport in silicate glasses. I. Localized phonons

George S. Dixon, Brent D. Gault, Shu-yun Shi, Patricia A. Watson, and James P. Wicksted
Department of Physics, Oklahoma State University, Stillwater, Oklahoma 74078
(Received 8 June 1993)

Measurements of the thermal diffusivities between 80 and 500 K for five silicate glasses of composition $0.15(M_2O)0.05(ZnO)0.05(BaO)0.05(Eu_2O_3)0.70(SiO_2)$, where M is Li, Na, K, Rb, or Cs are presented. In each case the thermal diffusivity asymptotically approaches a linear temperature dependence at high temperatures. The data are analyzed using a model that contains extended phonons and, above a mobility edge, localized phonons that participate in the transport through thermally activated hopping. The lowest-frequency Raman peak is used as a quantitative measure of the mobility edge. The thermally averaged relaxation times that characterize the localized-mode and extended-mode contributions to the thermal diffusivities are studied as functions of the mobility edge across this isostructural series of glasses.

INTRODUCTION

Thermal transport properties of glasses have presented an interesting set of research questions over the last two decades. The thermal conductivity experiments of Zeller and Pohl[1] initiated a train of investigation that culminated in the two-level-system (TLS) model[2,3] which accounts for many of the properties[4] of glasses at temperatures below the plateau region. In this picture the heat carriers are extended-state phonons, similar to the Debye phonons of crystalline solids, and the TLS provide a scattering mechanism for them. On a more general level, an important consequence of the success of the TLS model has been the recognition that amorphous solids can support excitations that differ qualitatively, as well as quantitatively, from those ordinarily encountered in crystalline solids.

At temperatures above the plateau, there is not yet consensus on the nature of the phonons that provide the heat carriers nor on the elastic properties of the glass that may be needed for effective thermal transport by these modes. The most successful current models hypothesize that the phonons are weakly localized by the disordered structure of the glass. The thermal transport process is one in which these localized phonons diffuse among neighboring localization sites by a random walk or hopping process. Cahill and Pohl[5] have used such a random walk model in which the localized phonons have a strong, temperature-independent damping and diffuse among equivalent sites to account for the thermal conductivities of a number of simple glasses. Their model predicts that the thermal transport coefficients will become independent of temperature once the glass is at a sufficiently high temperature that equipartition applies. Orbach and coworkers[6–8] have developed a model in which the localized phonons (fractons) execute thermally activated hopping among inequivalent localization sites. We shall refer to this as the thermally activated hopping (TAH) model. This model predicts that the thermal transport coefficients will be proportional to T at high temperatures. This result was not seen in the high-temperature limit for the simple glasses analyzed by Cahill and Pohl as these have thermal conductivities that tend toward a limiting value at the upper extreme of the temperature range in their data. The TAH model has also been controversial because of its use of a fractal mesoscale structure for the glass to facilitate computation.

In the present paper we shall present measurements of the thermal diffusivities between 80 and 500 K for five related silicate glasses having the composition

$$0.15(M_2O)0.05(ZnO)0.05(BaO)0.05(Eu_2O_3)0.70(SiO_2)\ ,$$

where the network modifier M is an alkali metal. We shall show that these results can be adequately described by a TAH model with localized phonons as the principal heat carriers in this temperature range. The model that we use employs many of the ideas inherent in the fracton model[6–8] without explicit reference to the mesostructure of the glasses. While this is somewhat limiting in terms of first-principles computational ability, we shall rely on empirical properties of the glasses to support the analysis. Extended phonons will also be seen to make a small but important contribution to the transport in these glasses. In the following paper (herein referred to as II) results will be presented for a second set of network-modified silicate glasses in which it is necessary to include a significant contribution of the extended-state phonons to account for the thermal transport. It will also be shown there that this picture provides good agreement with the thermal diffusivity of fused silica and thus provide a connection between the Cahill and Pohl and the TAH pictures of the transport process.

EXPERIMENTAL

Thermal diffusivity is a technique of preference for studying thermal transport in poor heat conductors because of its insensitivity to radiative heat losses. The thermal diffusivities were measured using an adaptation of the transient technique developed by Kennedy *et al.*[9,10] Figure 1 shows a block diagram of our apparatus. The samples, kindly given to us by Powell, were

0163-1829/94/49(1)/257(8)/$06.00

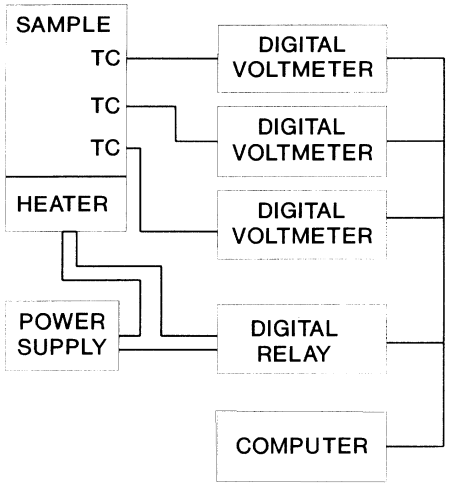

FIG. 1. Block diagram of the apparatus.

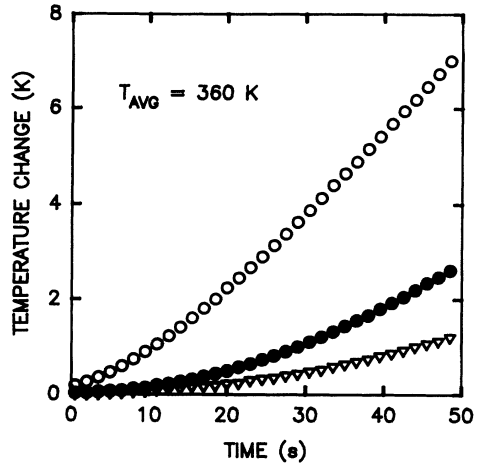

FIG. 2. Typical temperature vs time data. The upper curve is for the thermometer closest to the heater and the lower curve is for the thermometer farthest from the heater. These data are for the K-modified glass.

rectangular parallelepipeds, typically $3\times3\times15$ mm^3. Shallow grooves spaced at 5.0-mm intervals were cut into the sample to hold the three thermometers. These were 0.025-mm-diam chromel-alumel thermocouples referenced to electronic ice points. The thermocouples were anchored to the sample with a small amount of thermally conducting paste (an alumina-filled silicone grease). With this same thermal compound, the sample base was attached to a resistance heater used to obtain a transient temperature distribution in the specimen. For measurements above room temperature this assembly was mounted in a small tube furnace that controlled the mean temperature of the sample. Low-temperature measurements were obtained with this assembly mounted on the cold finger of a liquid-nitrogen cryostat.

The experiment was carried out under microcomputer control with the instruments communicating over an IEEE-488 interface bus. Simultaneous readings of the three thermometers were obtained by sending a group trigger command to the digital voltmeters. Each of these was a Hewlett-Packard model 3478A digital multimeter having a sensitivity of 0.1 μV. With the sample in steady-state conditions temperature readings were taken to establish a "baseline" for the measurement. On command from the computer, the digital relay was closed, supplying current to the transient heater. This current was maintained constant while simultaneous temperature measurements were taken by the three thermometers at intervals of 0.5 s. These data were collected for an elapsed time of 50–100 s. During this time a temperature change of 3–7 K occurred at the thermometer closest to the heater. At the end of this data-collection interval the relay was opened to turn off the transient heater and allow steady-state conditions to become reestablished. Figure 2 displays a typical data set of temperatures as functions of time for one of our glasses.

The thermal diffusivity, α, can be obtained from these data via the diffusion equation,

$$\frac{\partial T}{\partial t}=\alpha\nabla^2 T \ . \tag{1}$$

Kennedy, Sidles, and Danielson[9] used trial values of the thermal diffusivity to solve the diffusion equation using a mesh method. We have instead used a simple algorithm for the diffusivity that could be evaluated in a few seconds by the microcomputer. Under the assumption of one-dimensional heat flow, $\nabla^2 T$ was estimated by the finite difference relation for each measurement time in the data set. Here L, M, and U refer to the lower, middle,

$$\nabla^2 T_M \approx [(T_U - T_M)-(T_M - T_L)]/(\Delta x)^2 \ , \tag{2}$$

and upper thermometers, respectively, and Δx is the spacing between adjacent thermometers. At each time t_j, $\partial T(t_j)/\partial t$ was estimated by fitting a regression line to a short segment of $T_M(t)$ on either side of t_j and using the slope of this line as the estimate of the time derivative. Typically segments of eight points were used in this procedure. The estimates of $\nabla^2 T_M$ were refined by averaging over the same time interval used to evaluate the time derivative. According to (1), $\partial T_M/\partial t$ should be a linear function of $\nabla^2 T_M$ with slope α. Figure 3 illustrates the result of this procedure applied to the data set displayed in Fig. 2. The curve is remarkably linear, particularly in view of the number of numerical derivatives that have been performed to generate it. Through the use of this algorithm, both η and plots of the data in the form of Figs. 2 and 3 are available to the experimenter in essentially real time. The value of α obtained in this way was assigned to the mean temperature of the middle thermometer during the measurement cycle.

Two kinds of checks have been performed on the reliability of this algorithm to represent the diffusion equation faithfully. First, the method has been used to measure the thermal diffusivities of several standard samples, including fused silica (to be discussed in II), whose known thermal diffusivities cover a broad range of values and which include both amorphous and crystalline solids. In all cases the thermal diffusivities measured by the present technique were in excellent agreement with those report-

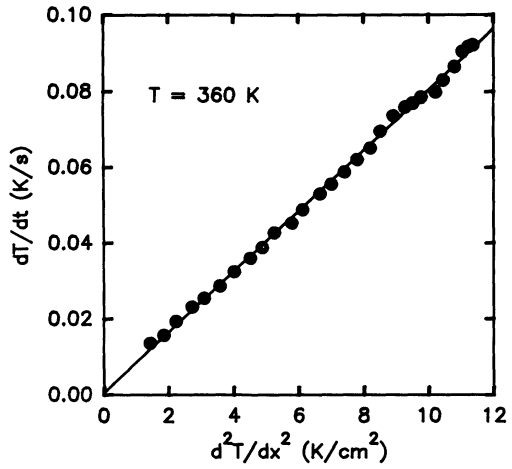

FIG. 3. Plot of $\partial T/\partial t$ vs $\partial^2 T/\partial x^2$ calculated from the data of Fig. 2 as described in the text. The slope of this line is the thermal diffusivity.

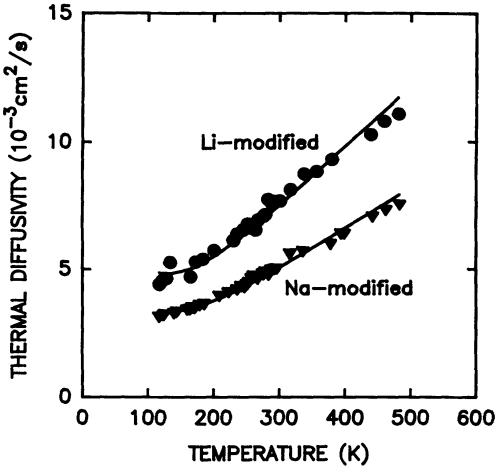

FIG. 4. Thermal diffusivities as a function of temperature for the Li-modified and Na-modified glasses. The curves are fits to the data using the model described in the text.

ed in the literature. A second test was performed on every data set to ensure that the smoothing procedure in our algorithm did not materially affect the estimated thermal diffusivity. In this test $\partial T_M(t_j)/\partial t$ was calculated by using the slope of the line connecting the two points $T_M(t_{j-1})$ and $T_M(t_{j+1})$. This, of course, produces the maximum scatter in the data. At each time in the measurement cycle η was evaluated, and the average of these values was computed. If this did not agree with the value obtained using the smoothing procedure, the data set was deemed too noisy to be useful.

Since the temperature was observed at only three locations along the length of the sample, finite difference procedures could not faithfully track $\nabla^2 T$ unless the contributions to the transient temperature distribution from higher-order derivatives of the temperature and from radial heat flow were small. This could be guaranteed only if the initial condition of the sample was near to steady state. In our apparatus the best results for these samples were obtained if the transients were allowed to dissipate to 20–30 min between data sets.

RESULTS AND DISCUSSION

Data are shown in Figs. 4–7 for each of the five glasses in this study. In each case the thermal diffusivity is a nearly linear function of temperature with a nonzero intercept. The slopes are quite similar for the glasses within this family. Each figure also exhibits a fit to the data using the model described below.

In Table I, we give some relevant physical properties for the glasses. We have also introduced the concept of a "formula unit" for the glasses. This useful concept is somewhat ill defined since these glasses are mixtures rather than compounds. We shall retain the quotation marks as a reminder of this. N_0 is the smallest number of atoms in which each element is represented in the same proportions as in the overall sample, and thus comprises one "formula unit." For these glasses $N_0=60$. The mass M is the mass of one "formula unit." The "molar volume" is the ratio of the density to M. The "molar radius" r_f is the radius of a sphere whose volume is the "molar volume."

It is also of interest to compare the magnitudes of the thermal diffusivities of these network-modified glasses to that of fused silica. Between 300 and 500 K the thermal diffusivity of fused silica has a nearly constant value of 9×10^{-3} cm^2/s. Both the Li-Zn-Ba-Eu silicate and the Cs-Zn-Ba-Eu silicate substantially exceed this value at temperatures above 400 K.

The linear temperature dependence observed for these samples is suggestive of transport by thermal activation of localized phonons similar to that described in the fracton model[6–8] by Orbach *et al.* However, we have insufficient knowledge of the mesoscale structure of these glasses to determine whether or not a fractal structure is appropriate. Fortunately, many of the features of the TAH model do not require the dilation symmetry of frac-

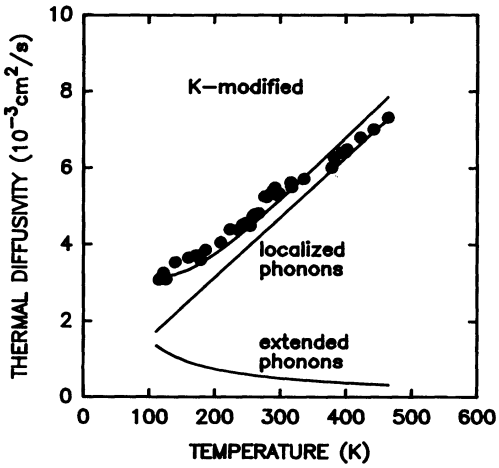

FIG. 5. Thermal diffusivity of the K-modified glass as a function of temperature. The curve is the fit to the data using the model described in the text. The separate contributions of extended phonons and localized phonons are also shown.

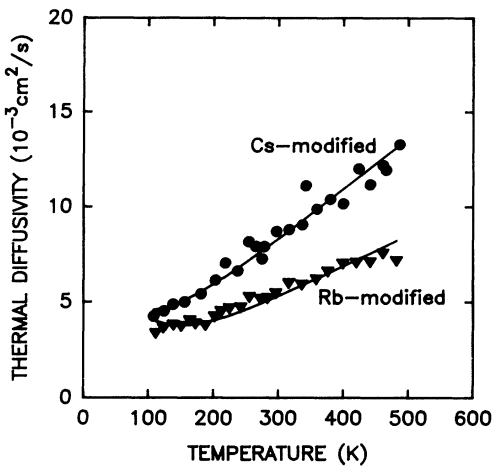

FIG. 6. Thermal diffusivities of the Rb-modified and Cs-modified glasses as function of temperature. The curves are fits to the data using the model described in the text.

tal structures. For our present purposes it is convenient to consider a broader class of TAH models of which the fracton model is a specific example. While this limits our potential for relating the parameters of the model to first principles, it avoids making possibly controversial assumptions about the structure. Thus, we shall postpone until a future paper such structural questions and treat thermally activated hopping transport in a form that involves parameters which we can estimate empirically.

There are two basic ingredients of the TAH model.

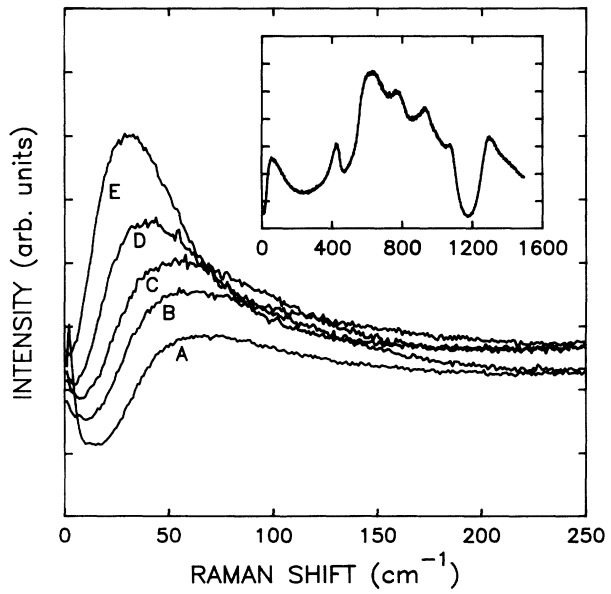

FIG. 7. Raman spectra of the glasses. The main figure shows the region of the boson peak. Curve *A* is the LI-modified glass; curve *B* is the Na-modified glass; curve *C* is the K-modified glass; curve *D* is the Rb-modified glass; and curve *E* is the Cs-modified glass. The inset shows the Raman spectrum of the Na-modified glass from 0 to 1600 cm^{-1}; the behavior of the other glasses is similar on this scale. All Raman spectra were obtained at room temperature.

The first is a phonon spectrum of the glass containing both low-frequency extended phonons and localized phonons above a minimum frequency ω_c, the phonon mobility edge. It is also necessary that there be significantly anharmonic forces to provide the thermal activation of the localized phonons. Rather than obtaining this from a calculation, we shall use empirical evidence to argue that this is the case for the glasses we study here.

A Brillouin scattering study[11] of these glasses found narrow peaks for the longitudinal and transverse phonons, indicating the presence of extended phonons with well-defined wave vectors at room temperature. A Raman scattering study[12] shows an onset of Raman activity for these glasses beginning at 10–20 cm^{-1} with a low-frequency peak, the "boson peak," in the 30–80 cm^{-1} range. This shows that the wave vectors are no longer well defined above this frequency. On general theoretical grounds one expects extended phonons with wave vector q such that q^{-1} is comparable to, or less than, ξ_c, the scale of the disorder in the network, to be strongly scattered by the inhomogeneities in density and elastic properties that will exist. Unless the mean free path Λ satisfies the Ioffe-Regel criterion, $q\Lambda > 1$, it is no longer possible to have a normal mode with this wave vector. Hence $q\xi_c \sim 1$ divides the low-frequency, extended states with reasonably well-defined wave vectors from higher-frequency modes for which the wave vector is no longer a good quantum number. Numerical studies of phonon wave vectors in disordered systems by Bell and Dean[13,14] indicate that this also signals the onset of phonon localization.

The broad homogeneous optical linewidths seen in rare-earth-modified glasses[15,16] indicate that the motions of the ligands due to phonons with such frequencies have large local amplitudes compared to crystalline solids where the homogeneous widths are orders of magnitude narrower. The amplitude of a localized phonon will be far larger than for an extended phonon of the same frequency because the phonon energy $\hbar\omega$ will be distributed over far fewer atoms (in a ratio $\sim l^3/V$, where V is the volume of the sample and l is the localization length for the phonon). The larger number of extended modes of frequency ω that are present at a given site only partially compensates for this since they add incoherently. This larger amplitude would also make anharmonicity more important for the localized modes than for extended modes with the same interatomic interactions. All this suggests to us that the phonons become localized at frequencies comparable to the onset of the Raman activity.

For these reasons, we shall interpret the onset of Raman activity in these glasses with phonon localization and take the maximum in the boson peak as representative of ω_c. The critical length ξ_c will be approximated by $2\pi v_s/\omega_c$, where v_s is the average sound velocity of the extended phonons. These, and other parameters associated with this interpretation, are given in Table II.

It is reasonable to expect that a set of glasses as closely related in composition as the ones studied here may also be structurally similar. This would imply that the critical length ξ_c should scale linearly with r_f, the radius of the "formula unit." The excellent agreement between experi-

TABLE I. Physical properties.

Alkali modifier	Li	Na	K	Rb	Cs
Formula mass (u)	1516	1612	1708	1987	2272
Density (g/cm^3)	3.22	3.21	3.15	3.47	3.74
Molar volume (nm^3)	0.786	0.839	0.906	0.956	1.015
Molar radius (nm)	0.573	0.585	0.600	0.611	0.623
Alkali ionic rad (nm)	0.06	0.095	0.133	0.148	0.169
Sound velocity[a] (10^5 cm/s)					
Transverse	3.31	3.07	2.91	2.74	2.54
Longitudinal	5.66	5.29	5.07	4.76	4.48
Mean	4.09	3.81	3.63	3.41	3.19
Raman frequencies[b] (cm^{-1})					
Boson peak	78	60	58	48	34
Other peaks	425	429	436	440	448
	625	637	606	600	599
	783	780	786	780	776
	948	932	930	940	929
	1076	1082	1087	1090	1086
	1328	1302	1295	1292	1303

[a]Reference 11.
[b]Reference 12.

ment and this relationship is exhibited in Fig. 8. This provides quantitative support for interpreting the boson peak as ω_c. Note, however, that this linear relation extrapolates to $\xi_c=0$ for $r_f>0$. This is minimum r_f corresponds closely to the radius of an equivalent number of units of crystoballite, to which the silica network would devitrify if it phase separated from the network modifiers; this is shown by the open circle in Fig. 8.

The leading contribution of the localized modes to thermal transport is a three-phonon anharmonic process illustrated schematically in Fig. 9. When a localized phonon decays, energy conservation requires that it reappear in some other mode elsewhere, a distance R away, in the glass. This is the process that we refer to as "hopping." This process will have significant probability of occurring only if there is substantial overlap of the donor and acceptor wave functions. Since there will be few other neighboring modes of exactly the same frequency, a low-frequency phonon will be emitted or absorbed to make up the energy difference between the donor and acceptor phonons. Extended phonons are likely candidates for these facilitator modes since they have access to the entire sample.

The hopping process contributes a thermal diffusivity given by

$$\alpha_{\rm loc}=\langle R^2\rangle/\tau_{\rm loc}\ , \tag{3}$$

where $\langle R^2\rangle$ is a thermally averaged square hopping distance and $\tau_{\rm loc}$ is the mean lifetime of the localized phonons. Since this process is facilitated by an extended phonon, the lifetime will be inversely proportional to the population of extended phonons

$$\tau_{\rm loc}\propto 1/n(\omega_c)\approx\hbar\omega_c/k_BT \tag{4}$$

when $k_BT\gg\hbar\omega_c$. $\langle R^2\rangle$ does not depend on temperature when T is large enough for equipartition to apply. In a series of glasses all having the same structure, $\langle R^2\rangle$ should scale with the size of the configuration as measured by r_f^2.

TABLE II. Transport parameters.

Alkali modifier	Li	Na	K	Rb	Cs
$\omega_c/2\pi$ (cm^{-1})	78	60	58	48	34
ξ_c (nm)	1.73	2.10	2.07	2.35	3.09
$C_{\rm ext}/C$ (high-T limit) (10^{-3})	3.53	2.12	2.39	1.72	0.797
B (10^{-5} cm^2/s K)	2.46	1.64	1.70	1.69	2.72
A (10^4 cm^2 K/s)	1.14	1.36	0.998	2.18	3.57
N_a/V (10^{19} cm^{-3})	21.5	12.1	12.6	8.62	3.77
$\langle R_{\rm min}\rangle$ (nm)	1.67	2.02	1.99	2.26	2.98
$\tau_{\rm loc}T$ (ns K)	1.13	2.49	2.33	3.03	3.27
$\tau_{\rm ext}T$ (ns K)	0.204	0.282	0.228	0.561	1.05
$\tau_{\rm loc}$ (300 K) (ps)	22.4	67.1	40.7	47.7	60.7
$\Lambda_{\rm ext}$ (300 K) (nm)	2.79	3.54	2.76	6.39	11.2

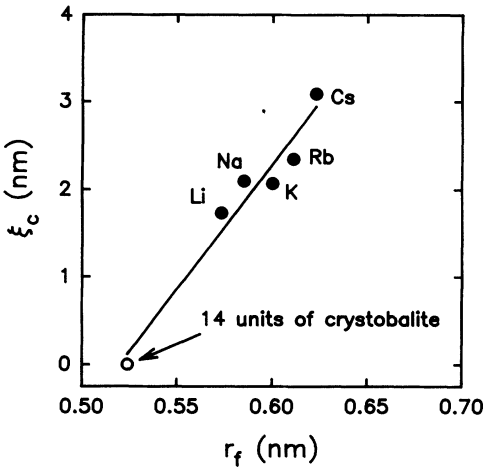

FIG. 8. Comparison of the critical length ξ_c calculated from the boson peak with the radius r_f of the "formula unit." The solid circles are the five glasses studied here. The open circle indicates r_f for the 14 SiO_2 units devitrified as crystabalite.

Thus, a phonon mobility edge and three-phonon anharmonic processes suffice to produce thermally activated hopping. The linear dependence of the thermal diffusivity on temperature is the signature of a significant transport due to thermally activated hopping and is not, of itself, an indication of a fractal glass. It is, short of access to the phonon wave functions, the best indication that phonon localization has occurred.

The extended phonons will also contribute to the thermal transport. Here one expects to be able to describe the conduction in the conventional phonon-gas picture. The net thermal conductivity is the sum of the contributions from the extended and the localized phonons,

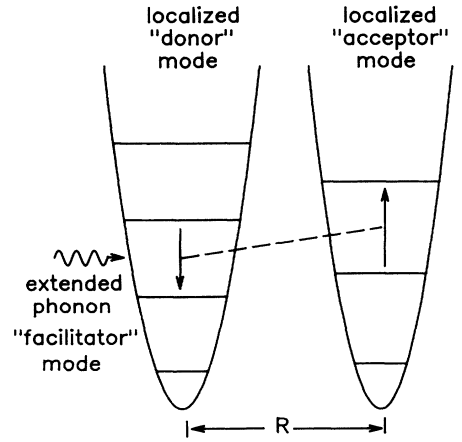

FIG. 9. Schematic representation of the thermally activated hopping process. The process deexcites a phonon in the donor mode and excites a phonon of different frequency on a neighboring acceptor mode. This is facilitated by an extended phonon to conserve energy. Note that the parabolas representing the localized mode potential wells are in normal coordinates while the separation R is in configuration coordinates.

$$\lambda=\tfrac{1}{3}C_{\rm ext}v_s^2\tau_{\rm ext}+C_{\rm loc}\langle R^2\rangle/\tau_{\rm loc}\ , \tag{5}$$

where $C_{\rm ext}$ and $C_{\rm loc}$ are the heat capacities per unit volume of the extended and localized phonons, respectively. The corresponding thermal diffusivity $\alpha=\alpha_{\rm ext}+\alpha_{\rm loc}$ is

$$\alpha=\frac{C_{\rm ext}}{3C}v_s^2\tau_{\rm ext}+\left[1-\frac{C_{\rm ext}}{C}\right]\langle R^2\rangle/\tau_{\rm loc}\ , \tag{6}$$

where $C=C_{\rm ext}+C_{\rm loc}$. At temperatures high enough for equipartition $C=3N_0k_B(\rho/M)$, where N_0 is the number of atoms in the "formula unit" and M is the mass of this unit. Using the Debye approximation to estimate the heat capacity of the extended phonons in this limit, $C_{\rm ext}=(\omega_c/v)^3k_B/(2\pi^2)$. The peaks in the Raman spectra, listed in Table I, extend to 1330 cm^{-1}. Therefore, it is necessary to correct for the temperature variation of the total heat capacity C. This has been done by approximating the phonon density of states by the center frequencies of the seven Raman peaks and using these in a multiterm Einstein approximation. The values for $C_{\rm ext}/C$ given in Table II are the values in the high-temperature limit. Note that the data used to estimate $C_{\rm ext}/C$ are not derived from the transport measurements.

The contribution of the extended phonons to the thermal transport in these glasses is too small to us unambiguously to extract the detailed behavior of $\tau_{\rm ext}$ from the data. However, the linear temperature dependence extending from 100 to 500 K suggests a strong anharmonicity. This indicates to us that the limiting relaxation time for the extended states will also be due to anharmonic, phonon-phonon processes. (In II a set of glasses will be studied in which a significant fracton of the transport is due to the extended phonons.) On the assumption that phonon-phonon scattering is the dominant resistive process for the extended phonons, we take $\tau_{\rm ext}\propto T^{-1}$ and fit the thermal diffusivity with a function of the form

$$\alpha=(C_{\rm ext}/C)AT^{-1}+(1-C_{\rm ext}/C)BT\ , \tag{7}$$

where A and B are constants to be determined from the fit. This relation has been used to analyze the thermal diffusivities for these glasses. The fitting coefficients are given in Table II. The results of this fit for each glass are displayed in Figs. 4–6. In Fig. 5, the separate contributions from the extended and localized phonons are displayed, as well, for the K-modified glass. It should be noted that it is also possible to represent the data using a $\tau_{\rm ext}$ that is independent of T.

In order for the localized phonons to be effective heat carriers the donor wave function must have substantial overlap with the acceptor wave function. For this reason it is of interest to estimate the minimum average distance between a donor and a neighboring acceptor. If $D(\omega)$ is the density of states of the localized modes, then the average number of acceptor modes per unit volume in the neighborhood of a donor of frequency ω_d will be

$$\frac{N_a}{V}=\int_{\omega_{\rm min}}^{\omega_{\rm max}}D(\omega)d\omega\ , \tag{8}$$

where $\omega_{\min}$ and $\omega_{\max}$ are the maximum and minimum localized phonon frequencies accessible by interaction with a single facilitator phonon. Although we do not know $D(\omega)$, the Debye approximation will suffice for an order-of-magnitude estimate. The density of acceptors will be smallest when the donor frequency is ω_c, giving $\omega_{\min}=\omega_c$ and $\omega_{\max}=2\omega_c$, assuming that the facilitators are the extended phonons. This gives

$$N_a/V=7/(2\pi)(\omega_c/v)^3 . \tag{9}$$

This allows us to estimate an average hopping distance to the nearest available acceptor for the phonons near the mobility edge as

$$\langle R_{\min}\rangle=(N_a/V)^{-1/3}\approx\xi_c , \tag{10}$$

which is comparable to the localization length for these phonons. Thus, the spatial distribution of acceptor modes with wave functions overlapping the donor wave function should be large enough that the hopping transport will not be bottlenecked by a lack of suitable acceptors provided the density of states for the localized phonons is not significantly less than a Debye density of states in the vicinity of the mobility edge.

Jagannathan, Entin-Wohlman, and Orbach[8] derive expressions for $\tau_{\rm loc}(\omega)$ and $\tau_{\rm ext}(\omega)$ for the process illustrated in Fig. 9 in the fracton approximation. The mean lifetimes obtained from these by thermal averaging and taking $\xi_c=2\pi v_s/\omega_c$ depend on ω_c, v_s, the density ρ, the anharmonic force constants $C_{\rm eff}$, and geometrical factors G.

$$\tau_{\rm loc}^{-1}=G_{\rm loc}C_{\rm eff}^2\omega_c^4T/(\rho^3v_s^9) , \tag{11}$$

$$\tau_{\rm ext}^{-1}=G_{\rm ext}C_{\rm eff}^2\omega_c^4T/(\rho^3v_s^9) . \tag{12}$$

The assumption of fractal geometry for the glass enters only in the details of the geometrical factors. This leads to the conclusion that if extended phonons provide the facilitator modes for the localized phonon transport, and this process also sets the mean free path of the extended phonons, then

$$G_{\rm loc}\tau_{\rm loc}=G_{\rm ext}\tau_{\rm ext} . \tag{13}$$

The experimental frequency dependence of the mean lifetimes of the localized and extended phonons can be estimated from the thermal diffusivities by

$$\tau_{\rm loc}=\langle R^2\rangle/\alpha_{\rm loc}\propto r_f^2/BT \tag{14}$$

using r_f to scale the hopping distance, and

$$\tau_{\rm ext}\approx\frac{3\alpha_{\rm ext}}{v_s^2C_{\rm ext}/C}\approx\frac{3A}{v_s^2T} . \tag{15}$$

This is a better estimate of the magnitude of $\tau_{\rm loc}$ than would be obtained by using $\langle R_{\min}\rangle$ for the hopping distance, since the latter represents the maximum distance at full localization while the measured diffusivity represents an average over all localized modes. It is also of interest to estimate the mean free path $\Lambda=v_s\tau_{\rm ext}$ for the extended phonons. Values for the magnitudes of the lifetimes and the mean free paths at 300 K are given in Table II. Note that $q\Lambda>1$ for the extended phonons and also $\omega\tau_{\rm loc}>1$ for the localized modes at this temperature, indicating that these states exist as well-defined excitations.

The estimates for the frequency dependence of the relaxation rates, in the scaled form $\tau^{-1}\rho^3v_s^9/T$, derived from our data using (14) and (15) are displayed in Fig. 10. For the extended phonons a quartic power law $\tau_{\rm ext-1}\propto\omega_c^4$ is indicated, as predicted by Jagannathan *et al.* This differs from the ω^3 frequency dependence observed for monochromatic, low-frequency phonons in fused quartz by Dietsche and Kinder.[17] The quartic power law suggests that the anharmonicity of the extended states is relatively insensitive to the change in the alkali modifier. The results of this analysis for $\tau_{\rm loc}^{-1}$ also show an ω_c^4 power law for the four glasses having the highest ω_c's. The Cs-modified glass deviates significantly from this behavior, its thermal diffusivity being too large to scale in this way. This increase in $\tau_{\rm loc}^{-1}$ from the expected proportionality for the lifetimes may indicate a stronger dependence of the anharmonicity of the localized states on the alkali modifier. However, one intuitively expects that the Li-modified glass, rather than the Cs-modified, would be more anharmonic. This is because of the larger amplitude that would be needed for a 78-cm^{-1} localized phonon as compared to lower frequencies and also because of the smaller size and mass of the Li. An alternate, more physically reasonable, possibility is that the hopping process may be facilitated by another mechanism that does not limit the mean free path of the extended phonons. We suggest that this may be due to low-frequency *localized* modes acting as facilitators as well as carriers. Their importance to the transport would be expected to increase as the mobility edge lowers and restricts the number of extended modes available. The low-frequency localized modes have been shown[18] to

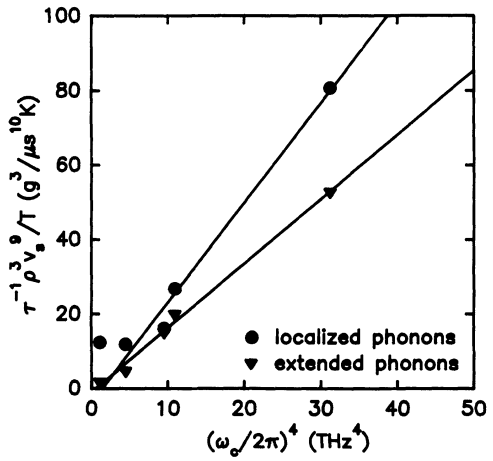

FIG. 10. Comparison of the scaled phonon relation rates for the localized states (circles) and the extended states (triangles). The lines are regressions to an ω_c power law with an exponent of 4.3 for the extended states for all five glasses and 4.1 for the localized states for the four glasses with the largest ω_c's. Note, however, the deviation of the localized phonon data from this behavior at the lowest frequency.

make a significant contribution to the related problem of phonon-assisted energy transfer among optically excited states of rare-earth ions in glasses.

Although the use of $\tau_{\rm ext}^{-1} \propto T$ to describe our data for these glasses leads to a result that agrees with the prediction of Jagannathan *et al.*, it is important over such a restricted interval of the temperatures studied here that, as we noted above, a temperature-independent relaxation rate for the extended states produces an equally good fit with the experiments. Our choice of this form is based on observations of a closely related family of silicate glasses, to be described in II, for which the thermal diffusivity sharply decreases with increasing temperature between 100 and 250 K before going over to the linearly increasing form that we have attributed to TAH at room temperature and above. Our argument for preferring phonon-phonon scattering in the present case is large anharmonicity indicated by the similarity in composition of the two families.

SUMMARY

The linear term in the temperature dependence of the thermal diffusivities of these glasses has been shown to provide experimental evidence for transport by localized phonons at frequencies above a mobility edge ω_c. The model used to describe the data is based on the ideas of the thermally assisted fracton hopping model, but does not assume or imply an underlying fractal mesostructure for the glass. At large values of the mobility edge, $\tau_{\rm loc}$ scales with $\tau_{\rm ext}$ for these for isostructural glasses. The mobility edge is associated in this relationship with the onset of Raman activity at low frequencies, thus implying that this onset is the result of phonon localization rather than merely the breakdown of wave-vector conservation. The localization length ξ_c derived from the Raman spectra and the sound velocities is a linear function of the radius of the most primitive "formula unit" for the composition of these glasses.

The relaxation times extracted from our thermal diffusivities show an $\omega_c^4 T$ dependence for both the localized and the extended phonons. This provides strong evidence that the TAH model is appropriate to the description of thermal transport in these glasses. These results do not, however, address the question of a possible underlying fractal mesostructure as used by Jagannathan, Entin-Wohlman and Orbach[8] as a computational aid in their theoretical study of this process. The Cs-modified member of this family exhibits a significantly larger thermal diffusivity than expected from the $\omega_c^4 T$ relation, suggesting that low-frequency localized phonons are also acting as facilitator modes for the hopping transport in this glass.

A significant practical result of the dominance of transport by this thermally activated hopping is that, other factors being equal, an increase in the anharmonicity in the network will increase its thermal diffusivity. This result, which is counterintuitive from our experience with the kinetic model for a phonon gas, comes from the consequent decrease in $\tau_{\rm loc}$ which increases the hopping rate. In the present family of glasses, the thermal diffusivities of both the Li-modified and Cs-modified members become larger than that of fused silica above room temperature. The scaling relation between r_f and ξ_c, illustrated in Fig. 8, may also allow the use of Raman and Brillouin scattering to assess the structural similarity of glasses having the same or closely related compositions.

This model for the thermal transport as due to contributions from localized and extended phonons provides a consistent picture of our data on this family of glasses. The two fitting parameters in the model vary across the family much as expected from other measured properties of these systems. Estimates of the phonon lifetimes, hopping distances, and mean free paths that needed to account for the results are physically reasonable. In II, a similar study on another family of glasses in which the extended phonons play a more significant role will be presented. The model will be shown to account well for that situation also.

ACKNOWLEDGMENTS

It is a pleasure to thank Richard Powell for these samples and numerous helpful discussions. We also appreciate the insights of George Gangwere and his permission to quote from his data. The support of the National Science Foundation is gratefully acknowledged.

[1]R. C. Zeller and R. O. Pohl, Phys. Rev. B **4**, 2029 (1971).
[2]P. W. Anderson, B. J. Halperin, and C. M. Varma, Philos. Mag. **25**, 1 (1972).
[3]W. A. Phillips, J. Low Temp. Phys. **7**, 351 (1972).
[4]For a review, see *Amorphous Solids,* edited by W. A. Phillips (Springer-Verlag, Berlin, 1981).
[5]D. G. Cahill and R. O. Pohl, Solid State Commun. **70**, 927 (1989).
[6]S. Alexander, C. Laermans, R. Orbach, and H. M. Rosenberg, Phys. Rev. B **28**, 4865 (1983).
[7]S. Alexander, O. Entin-Wohlman, and R. Orbach, Phys. Rev. B **34**, 2726 (1986).
[8]A. Jagannathan, O. Entin-Wohlman, and R. Orbach, Phys. Rev. B **39**, 13 465 (1989).
[9]W. L. Kennedy, P. H. Sidles, and G. C. Danielson, Direct Energy Conversion **2**, 53 (1962).
[10]G. C. Danielson and P. H. Sidles, in *Thermal Conductivity 2,* edited by R. P. Tye (Academic, London, 1989), p. 149.
[11]G. Gangwere, Ph.D. dissertation, Oklahoma State University, 1991 (unpublished).
[12]Details of the Raman measurements are planned to be published elsewhere.
[13]P. M. Selzer, D. L. Huber, D. S. Hamilton, W. M. Yen, and M. J. Weber, Phys. Rev. Lett. **36**, 813 (1976).
[14]G. Dixon, R. Powell, and X. Gang, Phys. Rev. B **33**, 2713 (1986).
[15]R. J. Bell, Rep. Prog. Phys. **35**, 1315 (1972).
[16]P. Dean, Rev. Mod. Phys. **44**, 127 (1972).
[17]W. Dietsche and H. Kinder, Phys. Rev. Lett. **43**, 1413 (1979).
[18]G. Dixon, J. Luminesc. **45**, 93 (1990).